Eur. Phys. J. C 46, 69–79 (2006)
Digital Object Identifier (DOI) 10.1140/epjc/s2006-02500-4

THE EUROPEAN PHYSICAL JOURNAL C

# Production properties of $K^{\star}(892)^{\pm}$ vector mesons and their spin alignment as measured in the NOMAD experiment

The Nomad Collaboration

A. Chukanov[6,a], D. Naumov[6,7], B. Popov[6,14], P. Astier[14], D. Autiero[8], A. Baldisseri[18], M. Baldo-Ceolin[13], M. Banner[14], G. Bassompierre[1], K. Benslama[9], N. Besson[18], I. Bird[8,9], B. Blumenfeld[2], F. Bobisut[13], J. Bouchez[18], S. Boyd[20], A. Bueno[3,24], S. Bunyatov[6], L. Camilleri[8], A. Cardini[10], P.W. Cattaneo[15], V. Cavasinni[16], A. Cervera-Villanueva[8,22], R. Challis[11], G. Collazuol[13], G. Conforto[8,21,†], C. Conta[15], M. Contalbrigo[13], R. Cousins[10], D. Daniels[3], H. Degaudenzi[9], T. Del Prete[16], A. De Santo[8,16], T. Dignan[3], L. Di Lella[8b], E. do Couto e Silva[8], J. Dumarchez[14], M. Ellis[20], G.J. Feldman[3], R. Ferrari[15], D. Ferrère[8], V. Flaminio[16], M. Fraternali[15], J.-M. Gaillard[1], E. Gangler[8,14], A. Geiser[5,8], D. Geppert[5], D. Gibin[13], S. Gninenko[8,12], A. Godley[19], J.-J. Gomez-Cadenas[8,22], J. Gosset[18], C. Gößling[5], M. Gouanère[1], A. Grant[8], G. Graziani[7], A. Guglielmi[13], C. Hagner[18], J. Hernando[22], D. Hubbard[3], P. Hurst[3], N. Hyett[11], E. Iacopini[7], C. Joseph[9], F. Juget[9], N. Kent[11], M. Kirsanov[12], O. Klimov[6], J. Kokkonen[8], A. Kovzelev[12,15], A. Krasnoperov[1,6], S. Lacaprara[13], C. Lachaud[14], B. Lakić[23], A. Lanza[15], L. La Rotonda[4], M. Laveder[13], A. Letessier-Selvon[14], J.-M. Levy[14], L. Linssen[8], A. Ljubičić[23], J. Long[2], A. Lupi[7], V. Lyubushkin[6], A. Marchionni[7], F. Martelli[21], X. Méchain[18], J.-P. Mendiburu[1], J.-P. Meyer[18], M. Mezzetto[13], S.R. Mishra[3,19], G.F. Moorhead[11], P. Nédélec[1], Yu. Nefedov[6], C. Nguyen-Mau[9], D. Orestano[17], F. Pastore[17], L.S. Peak[20], E. Pennacchio[21], H. Pessard[1], R. Petti[8,15], A. Placci[8], G. Polesello[15], D. Pollmann[5], A. Polyarush[12], C. Poulsen[11], L. Rebuffi[13], R. Renò[16], J. Rico[24], P. Riemann[5], C. Roda[8,16], A. Rubbia[8,24], F. Salvatore[15], O. Samoylov[6], K. Schahmaneche[14], B. Schmidt[5,8], T. Schmidt[5], A. Sconza[13], M. Sevior[11], D. Sillou[1], F.J.P. Soler[8,20], G. Sozzi[9], D. Steele[2,9], U. Stiegler[8], M. Stipčević[23], Th. Stolarczyk[18], M. Tareb-Reyes[9], G.N. Taylor[11], V. Tereshchenko[6], A. Toropin[12], A.-M. Touchard[14], S.N. Tovey[8,11], M.-T. Tran[9], E. Tsesmelis[8], J. Ulrichs[20], L. Vacavant[9], M. Valdata-Nappi[4,c], V. Valuev[6,10], F. Vannucci[14], K.E. Varvell[20], M. Veltri[21], V. Vercesi[15], G. Vidal-Sitjes[8], J.-M. Vieira[9], T. Vinogradova[10], F.V. Weber[3,8], T. Weisse[5], F.F. Wilson[8], L.J. Winton[11], B.D. Yabsley[20], H. Zaccone[18], R. Zei[16], K. Zuber[5], P. Zuccon[13]

[1] LAPP, Annecy, France
[2] Johns Hopkins Univ., Baltimore, MD USA
[3] Harvard Univ., Cambridge, MA, USA
[4] Univ. of Calabria and INFN, Cosenza, Italy
[5] Dortmund Univ., Dortmund, Germany
[6] JINR, Dubna, Russia
[7] Univ. of Florence and INFN, Florence, Italy
[8] CERN, Geneva, Switzerland
[9] University of Lausanne, Lausanne, Switzerland
[10] UCLA, Los Angeles, CA, USA
[11] University of Melbourne, Melbourne, Australia
[12] Inst. for Nuclear Research, INR Moscow, Russia
[13] Univ. of Padova and INFN, Padova, Italy
[14] LPNHE, Univ. of Paris VI and VII, Paris, France
[15] Univ. of Pavia and INFN, Pavia, Italy
[16] Univ. of Pisa and INFN, Pisa, Italy
[17] Roma Tre University and INFN, Rome, Italy
[18] DAPNIA, CEA Saclay, France
[19] Univ. of South Carolina, Columbia, SC, USA
[20] Univ. of Sydney, Sydney, Australia
[21] Univ. of Urbino, Urbino, and INFN Florence, Italy
[22] IFIC, Valencia, Spain
[23] Rudjer Bošković Institute, Zagreb, Croatia
[24] ETH Zürich, Zürich, Switzerland

Received: 11 December 2005 / Revised version: 31 January 2006 /
Published online: 13 March 2006 – 

**Abstract.** First measurements of $K^\star(892)^\pm$ mesons production properties and their spin alignment in $\nu_\mu$ charged current (CC) and neutral current (NC) interactions are presented. The analysis of the full data sample of the NOMAD experiment is performed in different kinematic regions. For $K^{\star+}$ and $K^{\star-}$ mesons produced in $\nu_\mu$ CC interactions and decaying into $K^0\pi^\pm$ we have found the following yields per event: $(2.6 \pm 0.2\,(\text{stat.}) \pm 0.2\,(\text{syst.}))\%$ and $(1.6 \pm 0.1\,(\text{stat.}) \pm 0.1\,(\text{syst.}))\%$ respectively, while for the $K^{\star+}$ and $K^{\star-}$ mesons produced in $\nu$ NC interactions the corresponding yields per event are: $(2.5 \pm 0.3\,(\text{stat.}) \pm 0.3\,(\text{syst.}))\%$ and $(1.0 \pm 0.3\,(\text{stat.}) \pm 0.2\,(\text{syst.}))\%$. The results obtained for the $\rho_{00}$ parameter, $0.40 \pm 0.06\,(\text{stat.}) \pm 0.03\,(\text{syst.})$ and $0.28 \pm 0.07\,(\text{stat.}) \pm 0.03\,(\text{syst.})$ for $K^\star(892)^+$ and $K^\star(892)^-$ produced in $\nu_\mu$ CC interactions, are compared to theoretical predictions tuned on LEP measurements in $e^+e^-$ annihilation at the $Z^0$ pole. For $K^\star(892)^+$ mesons produced in $\nu$ NC interactions the measured $\rho_{00}$ parameter is $0.66 \pm 0.10\,(\text{stat.}) \pm 0.05\,(\text{syst.})$.

**PACS.** 13.15.+g; 13.60.Le; 13.87.Fh; 13.88.+e; 14.40.Ev

## 1 Introduction

Following the analyses of strange particles in neutrino interactions reported earlier [1–4] we present a study of the production properties of $K^\star(892)^\pm$ vector mesons observed through the $K^0_S\pi^\pm$ decay modes. The full data sample of the NOMAD experiment divided into subsamples of neutrino charged current (CC) and neutral current (NC) interactions is used for this analysis.

For the first time in neutrino experiments the acquired statistics of the $K^\star(892)^\pm$ mesons allows the measurement of the absolute and relative yields, the determination of their dependence on relevant kinematic quantities as well as the extraction of the spin alignment of these vector mesons.

### 1.1 $K^\star(892)^\pm$ production in neutrino interactions

In $\nu_\mu$ CC interactions with nucleons, in a dominant number of cases the produced $u$-quark is in a 100% left-polarized state, and it can eventually fragment into a $K^{\star+}(u\bar{s})$ vector meson ($J^P = 1^-$): $\nu_\mu N \to \mu^- K^{\star+} X$. The $K^{\star+}$ mesons containing the leading $u$-quark populate the current fragmentation region (the $x_F > 0$ region[1]). However, according to the LUND model [5] predictions this population is of the same order of magnitude as the fraction of $K^{\star+}$ mesons produced more centrally in the string fragmentation process, as seen in Fig. 1 *(left)*. It is therefore interesting to study the spin alignment in different kinematic regions, not only to relate a possible effect to a well defined initial state (at large $x_F$), but also to improve our knowledge of the spin transfer in the string fragmentation process. This is the main production mechanism for the $K^{\star-}$ mesons as seen in Fig. 1 (right).

Let us stress that neutrino NC interactions are different from CC interactions at the quark level: for example, a leading down quark, a leading up quark and even a leading strange quark can be produced in $\nu$ NC interactions.

### 1.2 Spin-related production properties of vector mesons

The production and decay properties of mesons carrying spin are described in terms of the spin density matrix $\rho_{mm'}$, where $m$ and $m'$ label the spin components along the quantization axis. The Hermitian $3 \times 3$ matrix $\rho$ with unit trace is built as a direct product of the quark and antiquark spin states. This matrix is usually defined in the helicity basis. The diagonal elements $\rho_{00}$, $\rho_{11}$ and $\rho_{1;-1}$ describe the relative intensities of the 0, $+1$ and $-1$ spin states of the particle. It is common to refer to the situation with $\rho_{00} = 1/3$ as to the no spin alignment case, regardless of the values of $\rho_{11}$ and $\rho_{1;-1}$. Note that the spin alignment is not equivalent to the polarization in the conventional sense. For example, $\rho_{11} = \rho_{1;-1} = 1/2$ and $\rho_{00} = 0$ is *unpolarized* but spin aligned. Further details about the spin density matrix can be found in [6].

The elements $\rho_{11}$ and $\rho_{1;-1}$ cannot be measured separately since vector mesons decay via strong interactions and therefore conserve parity. Thus, the spin alignment of a particle can only be studied through the diagonal element $\rho_{00}$. For $J^P = 1^-$ states it can be experimentally measured using the angular distribution of the meson decay products [7]:

$$W(\theta) = \frac{3}{4}\left[(1-\rho_{00}) + (3\rho_{00}-1)\cos^2\theta\right] , \qquad (1)$$

where $\theta$ is the angle between the direction of one of the decay products and the direction of the vector meson ($z$-axis) in its rest frame. The following are interpretations of some special cases for the $\rho_{00}$ parameter:

$\rho_{00} = \frac{1}{3}$ – no spin alignment; the probability of projections $+1$, $-1$ and 0 of the meson spin onto the $z$ axis are equal (in this case there is no dependence of (1) on $\cos\theta$);

$\rho_{00} = 0$ – spin alignment; only the $+1$ and $-1$ projections are possible;

$\rho_{00} = 1$ – spin alignment; only the 0 projection is possible.

[a] e-mail: chukanov@nusun.jinr.ru

[b] Now at Scuola Normale Superiore, Pisa, Italy

[c] Now at Univ. of Perugia and INFN, Perugia, Italy

[†] Deceased

[1] $x_F$ is defined as $x_F \equiv 2p_l^*/\hat{W}$, $p_l^*$ being the momentum of the vector meson along the $W$ boson direction and $\hat{W}$ the hadronic energy, both calculated in the hadronic centre of mass system.

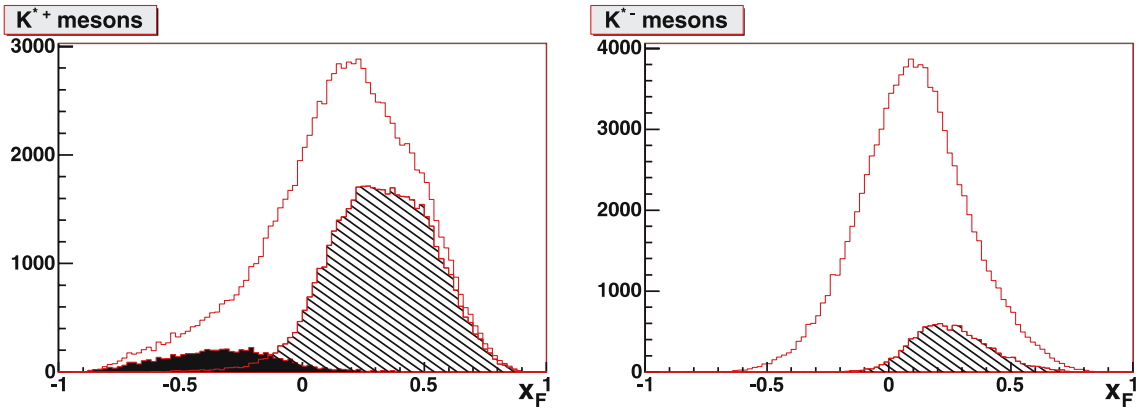


**Fig. 1.** $\nu_\mu$ CC interactions in the NOMAD experiment: LUND model predictions for the $x_F$ distribution of all $K^{\star+}$ (*left*) and $K^{\star-}$ (*right*) mesons, showing those originating from diquark fragmentation (*filled area*) and those originating from quark fragmentation (*hatched area*). The remainder of $K^{\star\pm}$ in the unshaded area come from string fragmentation

**Table 1.** The spin density matrix element $\rho_{00}$ as measured for different vector mesons

| Meson | Results (Experiment) | Comments |
|---|---|---|
| $\rho^{\pm}$ | $0.373 \pm 0.052$ (OPAL) | $0.3 < x_E < 0.6$ |
| $\rho^0$ | $0.43 \pm 0.05$ (DELPHI) | $x_E > 0.4$ |
| $\omega$ | $0.142 \pm 0.114$ (OPAL) | $0.3 < x_E < 0.6$ |
| $K^{\star 0}$ | $0.46 \pm 0.08$ (DELPHI) | $x_E > 0.4$ |
| | $0.66 \pm 0.11$ (OPAL) | $x_E > 0.7$ |
| $\phi$ | $0.54 \pm 0.06 \pm 0.05$ (OPAL) | $x_E > 0.7$ |
| | $0.55 \pm 0.10$ (DELPHI) | |
| $D^{\star\pm}$ | $0.40 \pm 0.02 \pm 0.01$ (OPAL) | $x_E > 0.5$ |
| $B^{*}$ | $0.32 \pm 0.04 \pm 0.03$ (DELPHI) | $0 < x_E < 1$ |
| | $0.33 \pm 0.06 \pm 0.05$ (ALEPH) | |
| | $0.36 \pm 0.06 \pm 0.07$ (OPAL) | |
| $K^{\star+}$ | $0.424 \pm 0.011$ (EXCHARM) | in the transversity |
| $K^{\star-}$ | $0.393 \pm 0.025$ (EXCHARM) | frame of $K^{\star}$ |
| $\rho^0$ | $0.65 \pm 0.18 \pm 0.10$ (BEBC, $\bar{\nu}$Ne) | $x_F > 0,\ z > 0.4$ |
| | $0.41 \pm 0.13 \pm 0.07$ (BEBC, $\nu$Ne) | |

### 1.3 Review of experimental results on $\rho_{00}$

The spin alignment of vector mesons was measured previously mainly in the LEP experiments in $e^+e^-$ annihilation at the $Z^0$ pole. A summary of available experimental results is given in Table 1. Spin alignment for the $\rho^0$, $\omega$, $K^{\star 0}$ and $D^{\star\pm}$ vector mesons was observed at high $x_E$, where $x_E$ is the ratio of the meson energy to the beam energy, and there was no spin alignment found for the $\rho^{\pm}$ and $B^{\star}$ mesons [8–10]. The EXCHARM collaboration observed spin alignment of $K^{\star\pm}$ mesons in neutron-carbon interactions in the transversity frame (the $z$-axis was defined to be normal to the production plane) of the $K^{\star\pm}$ at rest [11].

In a previous neutrino experiment the $\rho_{00}$ parameter of the $\rho^0$ vector meson was measured by the BEBC WA59 collaboration [12]. Large uncertainties do not allow to draw any conclusion about the spin alignment.

Note that a $3\sigma$ statistical significance for spin alignment is achieved only for $D^{\star\pm}$ mesons by the OPAL collaboration [10] and for $K^{\star+}$ mesons by the EXCHARM collaboration [11].

### 1.4 Theoretical predictions for the $\rho_{00}$ parameter

Different theoretical approaches (see for example [13, 14]) have been developed for the prediction of the $\rho_{00}$ parameter. All these models give a value of 1/3 for the $\rho_{00}$ parameter in the case of no spin alignment, but differ significantly in the treatment of the spin correlation mechanisms during the fragmentation process. For example, a model [15, 16] has been built to describe the results obtained in the LEP experiments (see previous subsection). This model can be used to predict the $\rho_{00}$ parameter dependence on $x_F$ in other vector meson production processes. In particular, this model predicts spin alignment of vector mesons produced in neutrino interactions in the NOMAD energy region [16]. These predictions for $\rho_{00}^V$ in $\nu_\mu p \to \mu^- V X$ at in-

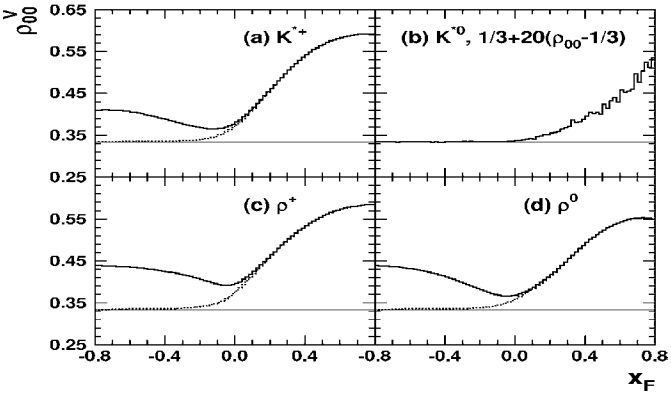


**Fig. 2.** The $\rho_{00}^V$ parameter in $\nu_\mu p \to \mu^- V X$ at $E_\nu = 43.8$ GeV. The *solid line* represents the results where the contribution of target fragmentation is taken into account, while the *dotted line* represents the results where only the contribution of the current fragmentation is included. The *horizontal line* shows the no spin alignment case, $\rho_{00} = 1/3$

coming neutrino energy $E_\nu = 43.8$ GeV both in the current and target fragmentation regions are shown in Fig. 2.

## 2 Experimental Procedure

### 2.1 The NOMAD experiment

The main goal of the NOMAD experiment [17] was the search for $\nu_\mu \to \nu_\tau$ oscillations in a wide-band neutrino beam from the CERN SPS. This search used kinematic criteria to identify $\nu_\tau$ CC interactions [18] and required a very good quality of event reconstruction, in particular the ability to reconstruct individual particles. This has indeed been achieved by the NOMAD detector, and moreover, the large data sample collected during four years of data taking (1995-1998) has allowed for detailed studies of neutrino interactions. The full data sample, corresponding to about $1.3 \times 10^6$ $\nu_\mu$ CC interactions in the detector fiducial volume, is used in the present analysis. A complete reprocessing of the whole NOMAD data sample has been performed using improved reconstruction algorithms with respect to those used for the previous NOMAD publications related to the studies of strange particles [1–3]. In particular, the cut on the density of hits in the drift chambers has been removed (see discussion in [19]). The data are compared to the results of a Monte Carlo (MC) simulation based on modified versions of LEPTO 6.1 [20] and JETSET 7.4 [21] generators for neutrino interactions (with $Q^2$ and $W^2$ cut-off parameters removed, where $Q$ is the four-momentum transferred from the incoming neutrino to the target nucleon) and on a GEANT [22] based program for the detector response. The relevant JETSET parameters have been tuned in order to reproduce the yields of strange particles measured in $\nu_\mu$ CC interactions in NOMAD [1]. A detailed description of the tuning of the MC simulation program will be the subject of a forthcoming publication. To define the parton content of the nucleon for the cross-section calculation we use the fixed-flavour parameterization [23] in the NNLO approximation. We do not include the parton shower treatment from JETSET. The reinteractions of hadrons with surrounding nucleons in target nuclei are described within the DPMJET [24] package. For the analysis reported below we used a MC sample consisting of about 3 million $\nu_\mu$ CC events and 2.6 million $\nu_\mu$ NC events. The MC assumes no spin alignment ($\rho_{00} = 1/3$) for $K^\star$ mesons.

### 2.2 Signal extraction

The selection procedure for the $\nu_\mu$ CC and $\nu$ NC event samples has been described in [2, 4] and is used in the current analysis along with the additional cut on the total visible hadronic energy: $E_{jet} > 3$ GeV. For the $\nu_\mu$ CC sample a further cut, $Q^2 > 0.8\,\mathrm{GeV}^2$, is applied. We identified $8 \times 10^5$ $\nu_\mu$ CC events with efficiency $\epsilon_{\nu_\mu \mathrm{CC}} = (77.16 \pm 0.03)\%$ and $2.3 \times 10^5$ $\nu$ NC events with efficiency $\epsilon_{\nu \mathrm{NC}} = (67.94 \pm 0.03)\%$. The efficiencies are computed with the help of the MC and are defined as ratios of the number of events reconstructed and identified as $\nu_\mu$ CC (NC) to the number of simulated $\nu_\mu$ CC (NC) events. The errors include only statistical uncertainties. The contamination of NC events in the CC event sample is estimated to be less than 0.1%, while the CC contamination in the NC sample is estimated to be about 8% (see [4] for details).

The procedure for the $K^0_S$ and $K^\star$ signal extraction was described in [1, 2]. Here we present only those details relevant to the yield and spin alignment measurements.

The NOMAD experiment has observed an unprecedented number of neutral strange particle decays in a neutrino experiment [1]. These decays appear in the detector as a $V^0$-like vertex: two tracks of opposite charge emerging from a common vertex separated from the primary neutrino interaction vertex (see Fig. 3).

Since the NOMAD detector has limited possibilities to distinguish (anti)protons from pions in the momentum range relevant for this analysis, our $V^0$ identification procedure relied on the kinematic properties of a $V^0$ decay to reject $\Lambda$ and $\bar{\Lambda}$. In Table 2 we summarize the numbers of identified $K^0_S \to \pi^+\pi^-$ decays in $\nu_\mu$ CC and $\nu$ NC interactions as well as their identification and reconstruction efficiencies and purities evaluated with the help of the MC.

For the $K^\star$ signal extraction we built an invariant mass distribution of any $K^0_S$ + *charged track* system and fit it using the following relativistic Breit-Wigner function [25]:

$$BW(m) = \frac{\Gamma}{(m^2 - M_0^2)^2 + M_0^2\Gamma^2}\left(\frac{m}{q}\right), \qquad (2)$$

with

$$\Gamma = \Gamma_0 \left(\frac{q}{q_0}\right)^{2l+1} \frac{M_0}{m}$$

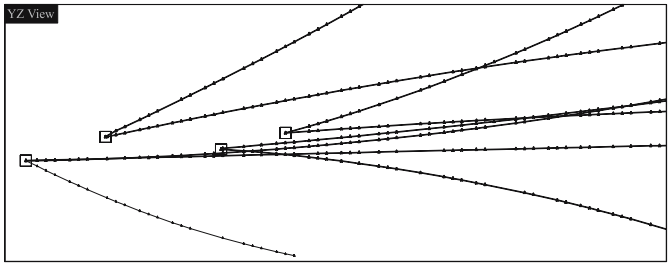


**Fig. 3.** A reconstructed data event containing 3 $V^0$ vertices identified as $K^0_S$ decays by the identification procedure. The scale on this plot is given by the size of the vertex boxes ($3 \times 3\,\mathrm{cm}^2$)

**Table 2.** Number of events, purity and efficiency of identified $K^0_S \to \pi^+\pi^-$ decays in $\nu_\mu$ CC and $\nu$ NC interactions in the data (efficiency includes the reconstruction and identification efficiencies of neutrino interactions)

| Sample | $N_{K^0_S}$ | $P_{K^0_S}(\%)$ | $\epsilon_{K^0_S}(\%)$ |
|---|---|---|---|
| $\nu_\mu$ CC | 14 280 | $97.1 \pm 0.1$ | $23.9 \pm 0.2$ |
| $\nu$ NC | 3718 | $96.8 \pm 0.1$ | $17.7 \pm 0.1$ |

where $M_0$, $\Gamma_0$ are the resonance mass and width, respectively, $q$ is the momentum of the decay product in the resonance rest frame ($q_0$ corresponds to $M_0$), and $l = 1$. We have chosen the following background (BG) parametrization:

$$\mathrm{BG} = a_1 \Delta^{a_2} e^{-(a_3\Delta + a_4\Delta^2)}, \tag{3}$$

where $\Delta = m - M_{\mathrm{th}}$, $M_{\mathrm{th}}$ being the threshold mass ($m_{K^0_S} + m_\pi$). The number of the $K^\star$ mesons extracted from the fit to the data (DATA) are given in Table 3 and Table 4.

In Fig. 4 and Fig. 5 we present the results of the signal extraction for both data and MC, for the selected $\nu_\mu$ CC and $\nu$ NC events respectively. Detailed information about extracted numbers of $K^{\star\pm}$ mesons in both the tuned MC and data for the $\nu_\mu$ CC and $\nu$ NC samples can be found in Table 3 and Table 4, where MC(true) is the total number of $K^\star \to K^0_S\pi$ decays in the fiducial volume in the MC sample, MC(rec) is the number of reconstructed $K^\star \to K^0_S\pi$ decays and MC(meas) is the number of decays, extracted from the fit. The ratio of MC(rec) to MC(true) determines the reconstruction efficiency $\epsilon_r$, while the ratio MC(meas) to MC(rec) determines the signal extraction efficiency $\epsilon_s$, which takes into account smearing effects due to momentum resolution. Both $\epsilon_s$ and $\epsilon_r$ were found very stable with respect to changes in MC tuning parameters (see paragraph Sect. 2.1).

### 2.3 Measurements of the $K^\star$ yields and determination of the $\rho_{00}$ parameter

The measured yield per $\nu_\mu$ CC (or NC) interaction for each $K^\star$ type that decays into $K^0\pi$ is defined as:

$$T_{K^\star} = \frac{N^{\mathrm{obs}}_{K^\star}}{\mathrm{Br}(K^0)\cdot\epsilon_{K^\star}} \cdot \frac{\epsilon_{\nu_\mu \mathrm{CC\ (NC)}}}{N_{\nu_\mu \mathrm{CC\ (NC)}}}, \tag{4a}$$

while the true number of $K^\star \to K^0\pi$ decays is given by:

$$N^{\mathrm{true}}_{K^\star} = \frac{N^{\mathrm{obs}}_{K^\star}}{\mathrm{Br}(K^0)\cdot\epsilon_{K^\star}}, \tag{4b}$$

where

- $N^{\mathrm{obs}}_{K^\star}$ is the number of $K^\star$ mesons obtained from the fit;
- $N_{\nu_\mu \mathrm{CC\ (NC)}}$ is the number of reconstructed $\nu_\mu$ CC (NC) events;
- $\epsilon_{\nu_\mu \mathrm{CC}}$ ($\epsilon_{\nu_\mu \mathrm{NC}}$) is the reconstruction and identification efficiency in the fiducial volume for $\nu_\mu$ CC (NC) events;
- $\mathrm{Br}(K^0) = 0.686/2$ is the branching ratio of $K^0_S \to \pi^+\pi^-$, where the factor of 2 reflects the observation of $K^0_S$ component only.

The combined efficiency $\epsilon_{K^\star}$ is given as a product of reconstruction efficiency ($\epsilon_r$) and signal extraction efficiency ($\epsilon_s$), see Table 3 and Table 4. The systematic uncertainties on these values with respect to changes in the selection criteria, are studied in the next subsection.

Note that for the neutral current interactions, formulae (4a) and (4b) should be modified because of ∼8% contamination from CC events in the $\nu$ NC sample [4]. This contamination is taken into account in the calculation of the $K^\star$ yields in the $\nu$ NC sample.

We have studied the $K^\star$ production properties in bins of several deep inelastic and fragmentation kinematic variables. The selection efficiency in each bin takes into account the migration of events accross these bins.

The $\rho_{00}$ parameter is determined from the fit of the $\cos\theta$ ($\theta$ is the angle between $K^*$ direction of flight and the direction of decay $\pi$ in the $K^*$ rest frame) distribution using the functional form given in (1).

In Fig. 6 we present the correlation between the simulated and reconstructed $\cos\theta$ variables for $K^{\star+}$ and $K^{\star-}$ produced in $\nu_\mu$ CC MC as well as for $K^{\star+}$ produced in $\nu$ NC MC interactions. The resolution in $\cos\theta$ is found to be better than 0.03 and does not depend significantly on the value of $\cos\theta$.

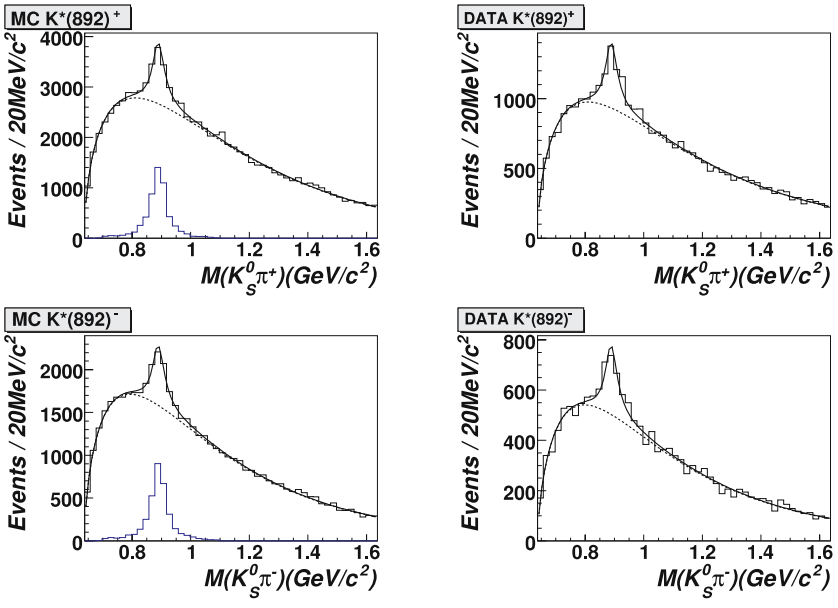


**Fig. 4.** $K^0_S$ + *positively charged track* (*top*) and $K^0_S$ + *negatively charged track* (*bottom*) invariant mass distributions for both MC (*left*) and data (*right*) for the $\nu_\mu$ CC sample. The MC plots show the expected signal peaks. *Solid line*: the result of the fit with signal and background, *dashed line*: only background

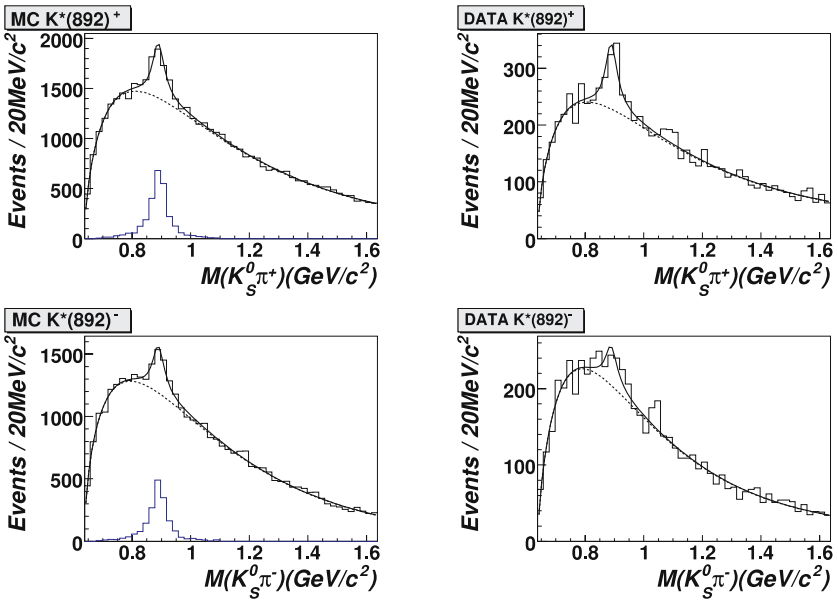


**Fig. 5.** $K^0_S + positively\ charged\ track$ (*top*) and $K^0_S + negatively\ charged\ track$ (*bottom*) invariant mass distributions for both MC (*left*) and data (*right*) for the $\nu$ NC sample. The MC plots show the expected signal peaks. *Solid line*: the result of the fit with signal and background, *dashed line*: only background

**Table 3.** $K^{\star+} \to K^0_S\pi^+$ and $K^{\star-} \to K^0_S\pi^-$ summary for $\nu_\mu$ CC interactions. The number of corresponding decays in the MC is normalized to the same number of $\nu_\mu$ CC events as in the real data sample

| | $N(K^{\star+} \to K^0_S\pi^+)$ | $N(K^{\star-} \to K^0_S\pi^-)$ |
|---|---|---|
| DATA | $1803 \pm 121$ | $1060 \pm 89$ |
| MC(meas) | $1846 \pm 80$ | $1066 \pm 61$ |
| MC(rec) | 2150 | 1374 |
| MC(true) | 9366 | 5612 |
| $\epsilon_r$ | $0.23 \pm 0.01$ | $0.24 \pm 0.01$ |
| $\epsilon_s$ | $0.86 \pm 0.04$ | $0.78 \pm 0.05$ |

**Table 4.** $K^{\star+} \to K^0_S\pi^+$ and $K^{\star-} \to K^0_S\pi^-$ summary for $\nu$ NC interactions. The number of corresponding decays in the MC is normalized to the same number of $\nu$ NC events as in the real data sample

| | $N(K^{\star+} \to K^0_S\pi^+)$ | $N(K^{\star-} \to K^0_S\pi^-)$ |
|---|---|---|
| DATA | $443 \pm 60$ | $197 \pm 53$ |
| MC(meas) | $385 \pm 26$ | $263 \pm 24$ |
| MC(rec) | 489 | 339 |
| MC(true) | 2689 | 1718 |
| $\epsilon_r$ | $0.18 \pm 0.01$ | $0.20 \pm 0.01$ |
| $\epsilon_s$ | $0.79 \pm 0.06$ | $0.78 \pm 0.08$ |

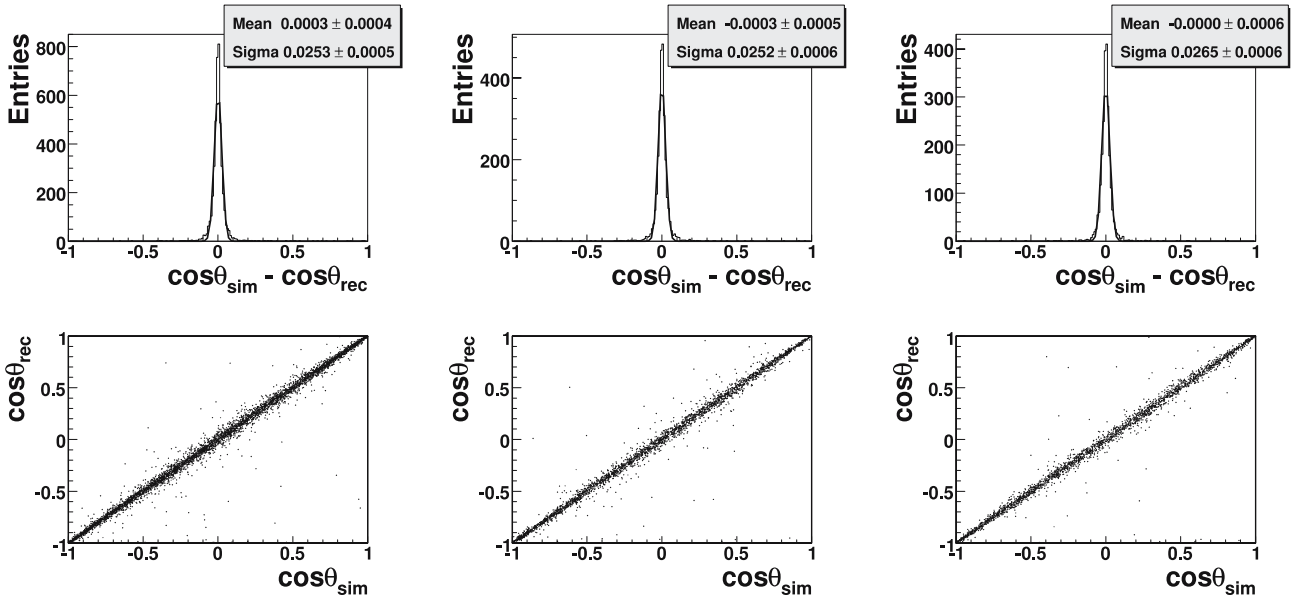


**Fig. 6.** Correlation between the simulated and reconstructed $\cos\theta$ variables for $K^{\star+}$ (*left*), $K^{\star-}$ (*middle*) produced in $\nu_\mu$ CC and for $K^{\star+}$ (*right*) produced in $\nu$ NC interactions

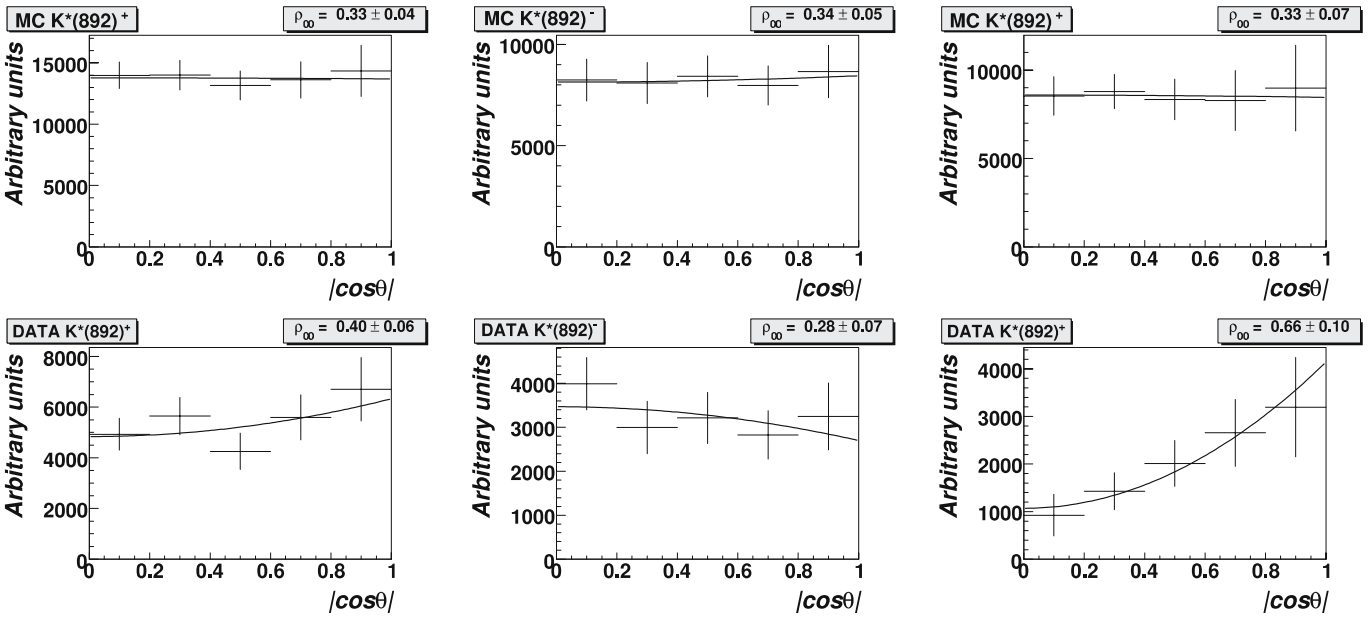


**Fig. 7.** Angular distributions of the pions from the decay of $K^\star(892)^+$ (*left*), $K^\star(892)^-$ (*middle*) for the $\nu_\mu$ CC sample and $K^\star(892)^+$ for the $\nu$ NC sample (*right*) for both MC (*top*) and data (*bottom*). Only statistical errors are shown

The $\cos\theta$ distributions for both data and MC for the $\nu_\mu$ CC and $\nu$ NC samples are presented in Fig. 7. The MC plots *(left)* confirm that the analysis procedure is self-consistent since we do not observe spin alignment in the MC ($\rho_{00} = 1/3$).

## 2.4 Systematic uncertainties

We have studied different sources of systematic uncertainties.

To investigate the dependence of the results on the $K^0_S$ selection criteria [2] we varied them within the following ranges (variations of these cuts correspond to changes of up to 6% in the statistics of the $K^0_S$ sample):

- cut on the transverse momentum of the pion from $K^0_S$ decay from 0.01–0.03 GeV/c (this cut can affect the contamination from "fake" $K^0_S$'s in the data). The default value is 0.02 GeV/c;
- cut on the $K^0_S$ momentum component perpendicular to the line connecting the primary and $V^0$vertices from 0.09–0.115 GeV/c (this cut affects mainly the contamination from secondary interactions). The default value is 0.1 GeV/c;
- cut on the $\chi^2$ probability of the $V^0$ vertex reconstruction changed from 0.005 to 0.035. The default value is 0.01;
- cut on the measured decay path of $K^0_S$ mesons varied from 12 to 30 cm. The default value is 16 cm.

We have also investigated the influence of the number of bins used in the invariant mass fit. The number of bins was changed to 40 and 70 (the default value is 50).

For the NC sample we varied the likelihood selection criteria [4] from 0 to 1 (the default value is 0.5).

We estimate the total systematic uncertainty as the sum in quadrature of the largest deviation with respect to the reference results in each of the above tests (neglecting possible correlations between different cuts).

In order to check for possible enhancements in the $K^\star$ signal region due to combinatorial effects as well as to validate the shape of the background distribution, we built the invariant mass of the $K^0_S$ + *charged track* system where the $K^0_S$ candidate and the *charged track* were taken from dif-

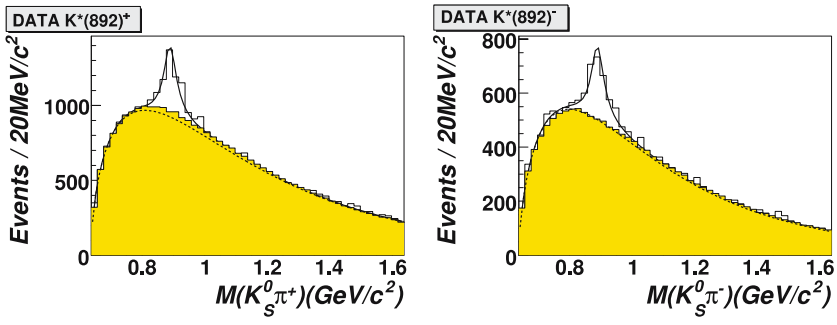


**Fig. 8.** $K^0_S$ + *positive charged track* (*left*) and $K^0_S$ + *negative charged track* (*right*) invariant mass distributions for the $\nu_\mu$ CC data sample. *Solid line*: the result of the fit with signal and background, *dashed line*: only background. Filled area shows the estimated background distribution when $K^0_S$ and *charged track* are taken from different events.

**Table 5.** The total numbers, absolute yields, relative yields and the $\rho_{00}$ parameter for $K^\star(892)^\pm$ mesons produced in $\nu_\mu$ CC and $\nu$ NC interactions that decay into $K^0\pi^\pm$ modes. Both statistical and systematic errors are shown

| Sample | Number of $K^\star$ | Yields of $K^\star$ (%) | $\frac{N(K^\star\to K^0\pi)}{N(K^0)}$ (%) | $\rho_{00}$ |
|---|---|---|---|---|
| $K^{\star+}$ CC | $26676 \pm 1784 \pm 1863$ | $2.6 \pm 0.2 \pm 0.2$ | $15.3 \pm 1.0 \pm 1.0$ | $0.40 \pm 0.06 \pm 0.03$ |
| $K^{\star-}$ CC | $16278 \pm 1372 \pm 500$ | $1.6 \pm 0.1 \pm 0.1$ | $9.4 \pm 0.8 \pm 0.3$ | $0.28 \pm 0.07 \pm 0.03$ |
| $K^{\star+}$ NC | $9024 \pm 1216 \pm 984$ | $2.5 \pm 0.3 \pm 0.3$ | $14.8 \pm 2.0 \pm 1.6$ | $0.66 \pm 0.10 \pm 0.05$ |
| $K^{\star-}$ NC | $3750 \pm 1012 \pm 762$ | $1.0 \pm 0.3 \pm 0.2$ | $6.1 \pm 1.7 \pm 1.2$ | – |

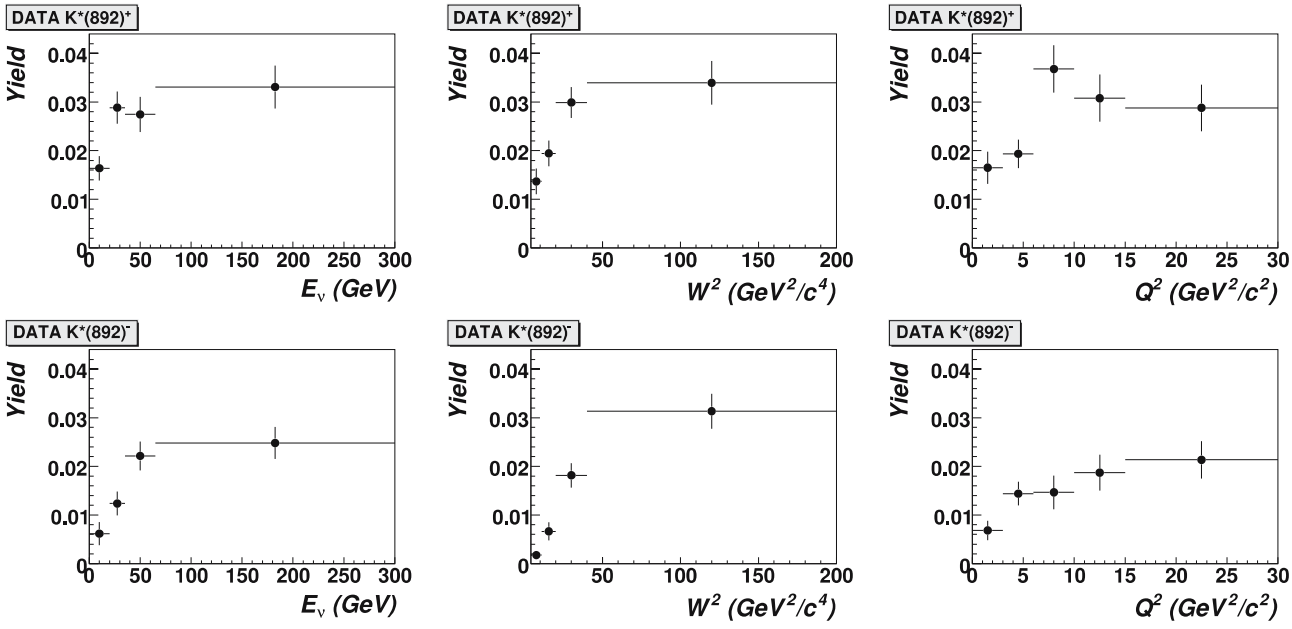


**Fig. 9.** Corrected $K^{\star+}$ (*top*) and $K^{\star-}$ (*bottom*) yields as a function of $E_\nu$, $W^2$, $Q^2$ in $\nu_\mu$ CC events. Only statistical errors are shown

ferent events, rotated such that the reconstructed hadronic momentum vectors coincided. Then the background was normalized to the invariant mass region above 1.1 GeV. The results are shown in Fig. 8. The shape of the background distribution is reasonably well described by the fitting procedure presented in Sect. 2.2.

## 3 Results

In this section we present the results for $K^\star(892)^\pm$ that decay into $K^0\pi^\pm$ modes.

Table 5 summarizes results for the total numbers, absolute yields, relative yields and the $\rho_{00}$ parameters for $K^\star(892)^\pm$ mesons in $\nu_\mu$ CC and $\nu$ NC interactions. As expected, the yields of $K^{\star+}$ mesons are larger than the yields of $K^{\star-}$ mesons in both $\nu_\mu$ CC and $\nu$ NC interactions. From this table one can conclude that the $\rho_{00}$ parameters for $K^{\star\pm}$ mesons produced in $\nu_\mu$ CC interactions are in agreement within statistical errors with the value of 1/3 which corresponds to the no spin alignment case. Also we observe that in $\nu$ NC interactions $K^{\star+}$ mesons are produced preferentially in the helicity zero state ($\rho_{00} > 1/3$), but the statistical errors are too large to reach a firm conclusion. For $K^{\star-}$ mesons produced in $\nu$ NC interactions the $\rho_{00}$ parameter could not be accurately determined because of the small statistics of the corresponding event sample.

In Sect. 3.1 and Sect. 3.2 we present the dependencies of the $K^\star(892)^\pm$ production yields and the $\rho_{00}$ parameter on different kinematic variables in $\nu_\mu$ CC interactions.

### 3.1 $K^{\star\pm}$ production yields

In Fig. 9 and Fig. 10 we show corrected $K^{\star\pm}$ yields in the data as a function of kinematic variables[2] $E_\nu$, $W^2$, $Q^2$, $x_{Bj}$, $y_{Bj}$ in $\nu_\mu$ CC events. The $K^{\star\pm}$ yields show a monotonic rise with $E_\nu$, $W^2$ and $Q^2$. From Fig. 10 we see that the dependence of the yields on the $x_{Bj}$ and $y_{Bj}$ vari-

[2] $x_{Bj}$ and $y_{Bj}$ are the standard Bjorken scaling variables.

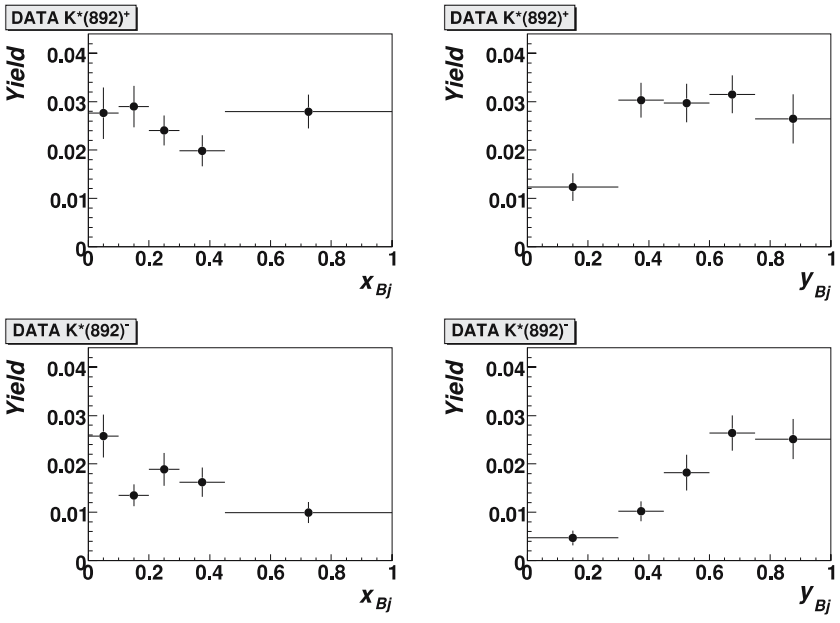


**Fig. 10.** Corrected $K^{\star+}$ (*top*) and $K^{\star-}$ (*bottom*) yields as a function of $x_{Bj}$, $y_{Bj}$ in $\nu_\mu$ CC events. Only statistical errors are shown

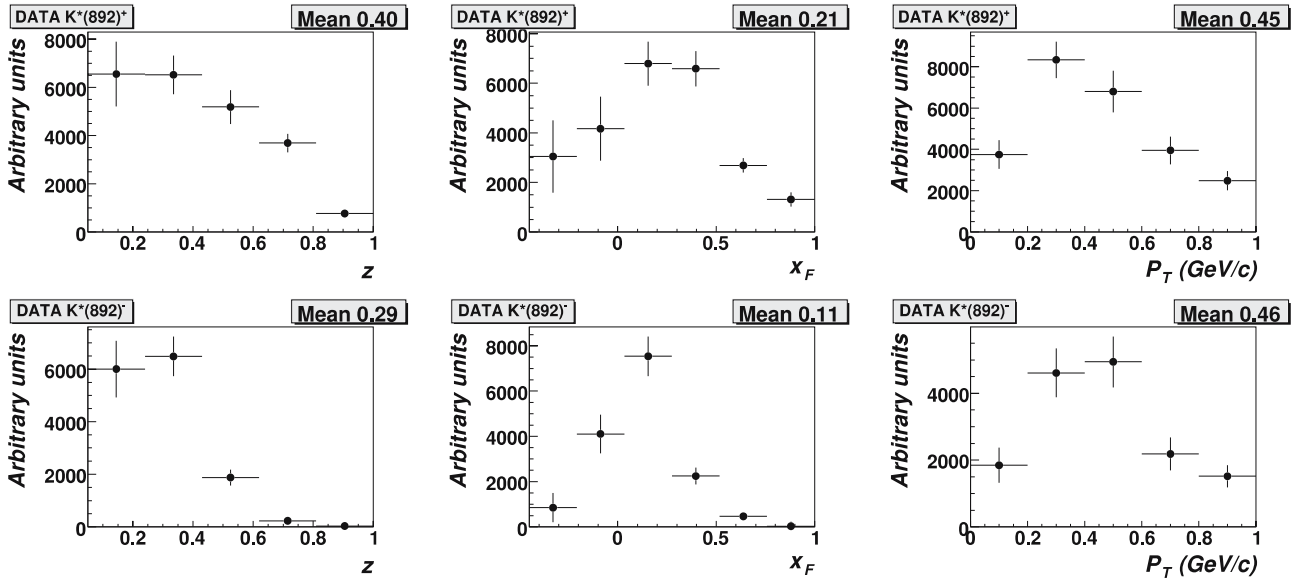


**Fig. 11.** Corrected $z$, $x_F$, $p_T$ distributions for $K^{\star+}$ (*top*) and $K^{\star-}$ (*bottom*) in $\nu_\mu$ CC events. Only statistical errors are shown

ables are different for $K^{\star+}$ and $K^{\star-}$ mesons. This fact could be explained by different production mechanisms ($K^{\star-}$ mesons are produced mainly from the string fragmentation processes while $K^{\star+}$ mesons are produced both from string fragmentation processes and from struck quark fragmentation).

$K^{\star\pm}$ distributions as a function[3] of $z$, $x_F$, $p_T$ are shown in Fig. 11. One can see a shift towards positive $x_F$ values in the distribution for $K^{\star+}$ mesons as compared to the distribution for $K^{\star-}$ mesons. In Fig. 12 we present the comparision of $x_F$ distribution for $K^{\star}$ mesons in MC and data.

### 3.2 The $\rho_{00}$ parameter of $K^{\star\pm}$ mesons

Figure 13 displays the $\rho_{00}$ parameter as a function of $z$, $x_F$, $p_T$ for $K^{\star+}$ *(left)* and $K^{\star-}$ *(right)*. The observed $x_F$ dependence does not seem to agree with the theoretical predictions of Ref. [15, 16].

The $\rho_{00}$ parameter has also been measured as a function of other kinematic variables ($E_\nu$, $W^2$, $Q^2$, $x_{Bj}$, $y_{Bj}$). Within the errors we do not observe any dependence on these variables.

[3] $z$ is the fraction of the total hadronic energy carried away by the $K^{\star\pm}$ in the laboratory system and $p_T$ is the transverse momentum the $K^{\star\pm}$ with respect to the hadronic jet direction.

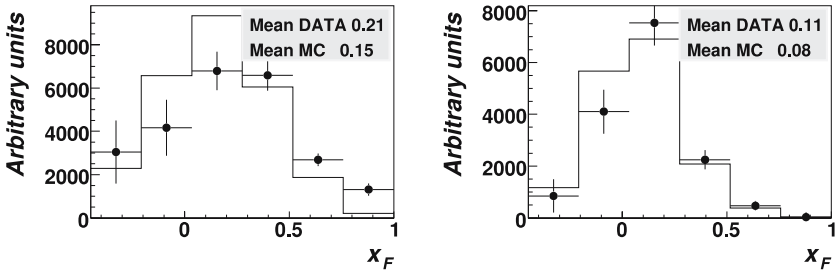


**Fig. 12.** Corrected $x_F$ distribution for $K^{\star+}$ (*left*) and $K^{\star-}$ (*right*) in MC (*histogram*) and data (*points with error bars*) $\nu_\mu$ CC events. Only statistical errors are shown

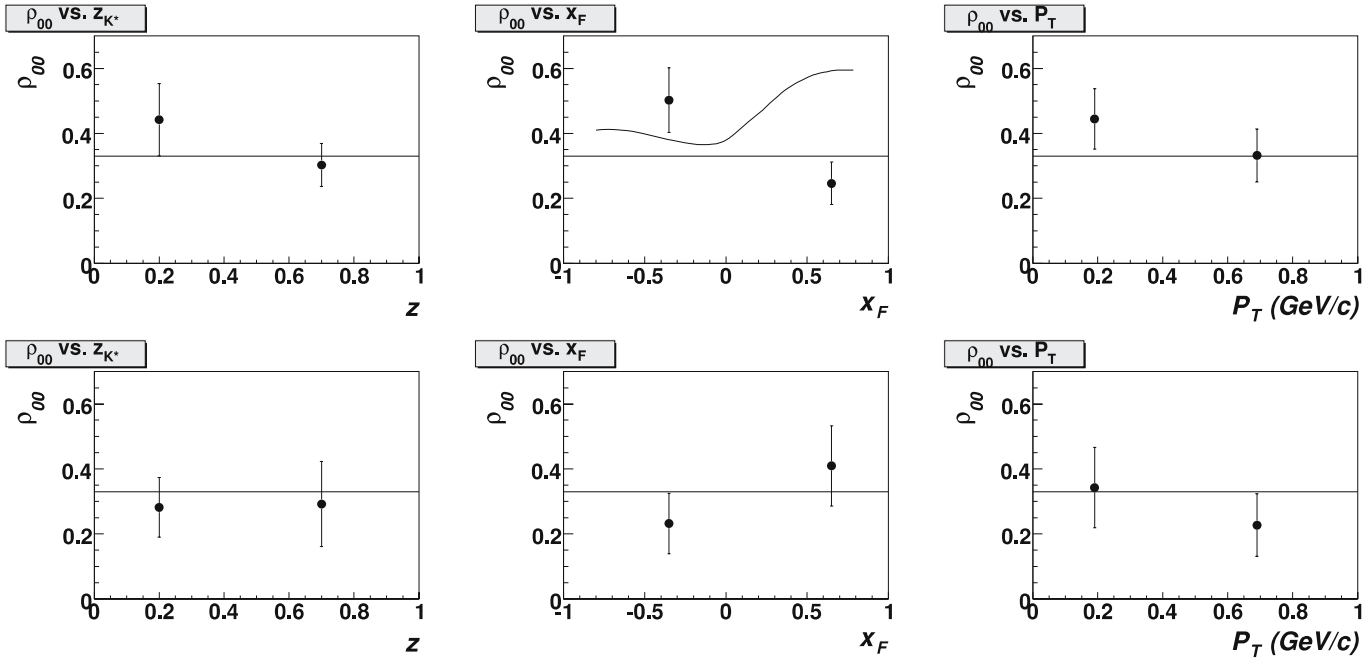


**Fig. 13.** The $\rho_{00}$ parameter as a function of $z$, $x_F$ and $p_T$ for $K^{\star+}$ (*top*) and $K^{\star-}$ (*bottom*) in the $\nu_\mu$ CC events. Only statistical errors are shown. The theoretical prediction [16] for the dependence of the $\rho_{00}$ parameter on $x_F$ for $K^{\star+}$ mesons is also shown.

## 4 Conclusion

In this analysis we have measured the production properties and spin alignment of $K^\star(892)^\pm$ vector mesons that decayed into $K^0_S\pi^\pm$ and were produced in $\nu_\mu$ CC and NC interactions in the NOMAD experiment.

For the first time in neutrino experiments the total yields of $K^{\star\pm}$ vector mesons that decayed into $K^0\pi^\pm$ modes have been measured. For the $K^{\star+}$ and $K^{\star-}$ mesons produced in $\nu_\mu$ CC interactions the following yields per event were found: $(2.6 \pm 0.2\,(\text{stat.}) \pm 0.2\,(\text{syst.}))\%$ and $(1.6 \pm 0.1\,(\text{stat.}) \pm 0.1\,(\text{syst.}))\%$ respectively, while for the $K^{\star+}$ and $K^{\star-}$ mesons produced in $\nu_\mu$ NC interactions the corresponding values are: $(2.5 \pm 0.3\,(\text{stat.}) \pm 0.3\,(\text{syst.}))\%$ and $(1.0 \pm 0.3\,(\text{stat.}) \pm 0.2\,(\text{syst.}))\%$. The yields of $K^{\star\pm}$ produced in $\nu_\mu$ CC interactions show a monotonic rise with the kinematic variables $E_\nu$, $W^2$ and $Q^2$.

The $K^{\star\pm}$ mesons $\rho_{00}$ parameters have been measured for the first time in neutrino experiments. The results obtained for the $\nu_\mu$ CC sample are in agreement within errors with the $\rho_{00} = 1/3$, which corresponds to no spin alignment for these mesons: $\rho_{00} = 0.40 \pm 0.06\,(\text{stat.}) \pm 0.03\,(\text{syst.})$ for $K^\star(892)^+$ and $\rho_{00} = 0.28 \pm 0.07\,(\text{stat.}) \pm 0.04\,(\text{syst.})$ for $K^\star(892)^-$. For $K^\star(892)^+$ mesons produced in $\nu$ NC interactios we observed an indication for preferential production in the helicity zero state ($\rho_{00} > 1/3$): $\rho_{00} = 0.66 \pm 0.10\,(\text{stat.}) \pm 0.05\,(\text{syst.})$, but the statistical errors do not allow us to reach a firm conclusion.

*Acknowledgements.* We gratefully acknowledge the CERN SPS accelerator and beam-line staff for the magnificent performance of the neutrino beam. The experiment was supported by the following funding agencies: Australian Research Council (ARC) and Department of Education, Science, and Training (DEST), Australia; Institut National de Physique Nucléaire et Physique des Particules (IN2P3), Commissariat à l'Energie Atomique (CEA), France; Bundesministerium für Bildung und Forschung (BMBF, contract 05 6DO52), Germany; Istituto Nazionale di Fisica Nucleare (INFN), Italy; Joint Institute for Nuclear Research and Institute for Nuclear Research of the Russian Academy of Sciences, Russia; Fonds National Suisse de la Recherche Scientifique, Switzerland; Department of Energy, National Science Foundation (grant PHY-9526278), the Sloan and the Cottrell Foundations, USA.

We also thank Liang Zuo-tang and Oleg Teryaev for valuable discussions.

## References


1. NOMAD Collaboration, P. Astier et al., Nucl. Phys. B **621**, 3 (2001)
2. NOMAD Collaboration, P. Astier et al., Nucl. Phys. B **588**, 3 (2000)
3. NOMAD Collaboration, P. Astier et al., Nucl. Phys. B **605**, 3 (2001)
4. NOMAD Collaboration, D. Naumov et al., Nucl. Phys. B **700**, 51 (2004)
5. B. Andersson, G. Gustafson, G. Ingelman, T. Sjöstrand, Phys. Rep. **97**, 31 (1983); T. Sjöstrand et al., Int. J. Mod. Phys A **3**, 751 (1988)
6. C. Bourrely, E. Leader, J. Soffer, Phys. Rep. **59**, 95 (1980)
7. J. F. Donoghue, Phys. Rev. D **17**,2922 (1978)
8. ALEPH Collaboration, D. Buskulic et al., Z. Phys. C **69**,393 (1995)
9. DELPHI Collaboration, P. Abreu et al., Phys. Lett. B **406**, (1997) 271; DELPHI Collaboration, P. Abreu et al., Z. Phys. C **68**, 353 (1995)
10. OPAL Collaboration, K. Ackerstaff et al., Phys. Lett. B **412**, 210 (1997); OPAL Collaboration, G. Abbiendi et al., Eur. Phys. J. C **16**, 61 (2000); OPAL Collaboration, K. Ackerstaff et al., Z. Phys. C **74**, 437 (1997)
11. EXCHARM Collaboration, A.N. Aleev et al., JINR preprint, **E1-99-178** (1999)
12. BEBC WA59 Collaboration, W. Wittek et al., Phys. Lett. B **187**, 179 (1987)
13. J. F. Donoghue, Phys. Rev. D **19**, 2806 (1979)
14. A.V. Efremov, O.V. Teryaev, Sov. J. Nucl. Phys. **36**, 557 (1982); A.V. Efremov, O.V. Teryaev, JINR preprint, **P2-82-832**, (1982)
15. Xu Qing-hua, Liu Chun-xiu, Liang Zuo-tang, Phys. Rev. D **63**, 111 301 (2001)
16. Xu Qing-hua, Liang Zuo-tang, hep-ph/0205291; Xu Qing-hua, Liang Zuo-tang, Phys. Rev. D **66**, 017 301 (2002)
17. NOMAD Collaboration, J. Altegoer et al., Nucl. Instr. and Meth. A **404**, 96 (1998)
18. NOMAD Collaboration, J. Altegoer et al., Phys. Lett. B **431**, 219 (1998); NOMAD Collaboration, P. Astier et al., Phys. Lett. B **453**, 169 (1999); NOMAD Collaboration, P. Astier et al., Phys. Lett. B **483**, 387 (2000); NOMAD Collaboration, P. Astier et al., Nucl. Phys. B **611**, 3 (2001)
19. NOMAD Collaboration, P. Astier et al. Phys. Lett. B **570**, 19 (2003)
20. G. Ingelman, LEPTO version 6.1, TSL-ISV-92-0065 (1992); G. Ingelman, A. Edin, J. Rathsman, LEPTO version 6.5, Comp. Phys. Comm. **101**, 108 (1997) [hep-ph/9605286]
21. T. Sjöstrand, LU-TP-95-20, (1995) [hep-ph/9508391]; T. Sjöstrand, Comp. Phys. Comm **39**, 347 (1986); **43**, 367 (1987)
22. GEANT: Detector Description and Simulation Tool, W5013, GEANT version 3.21
23. S. Alekhin, Phys. Rev. D **68**, 014 002 (2003)
24. J. Ranft, Phys. Rev. D **51**, 64 (1995); J. Ranft, arXiv:hep-ph/9911213; J. Ranft, arXiv:hep-ph/9911232
25. J.D. Jackson, Nuovo Cimento **34**, 1644 (1964)